Anti-Müllerian hormone induces autophagy to preserve the primordial follicle pool in mice

Tatiana Lecot-Connan, Yasmine Boumerdassi, Françoise Magnin, Nadine Binart, Peter Kamenický, Charlotte Sonigo, Isabelle Beau

Anti-müllerian hormone induces autophagy to preserve the primordial follicle pool in mice

Tatiana Lecot-Connan [1], Yasmine Boumerdassi [1], Françoise Magnin [1], Nadine Binart [1], Peter Kamenický [1, 2], Charlotte Sonigo [1, 3], Isabelle Beau [1]

[1] Physiologie et Physiopathologie Endocriniennes, Université Paris-Saclay, Inserm, 94276 Le Kremlin-Bicêtre, France

[2] Service d'Endocrinologie et des Maladies de la Reproduction, Hôpital Bicêtre, Le Kremlin-Bicêtre, France

[3] Service de Médecine de la reproduction et Préservation de la Fertilité, Hôpital Antoine Béclère, Clamart, France

Corresponding author :

Isabelle Beau

Inserm UMR-S 1185, faculté de Médecine Université Paris-Saclay

63 rue Gabriel Péri, 94276 Le Kremlin-Bicêtre, France

Phone: +33 1 49 59 66 29

Email: isabelle.beau@universite-paris-saclay.fr

Abstract

The reserve pool of primordial follicles (PMF) is finely regulated by molecules implicated in follicular growth or PMF survival. Anti-müllerian hormone (AMH), produced by granulosa cells of growing follicles, is known for its inhibitory role in the initiation of PMF growth. We observed in a recent *in vivo* study that injection of AMH into mice seemed to induce an activation of autophagy. Furthermore, injection of AMH into mice activates the transcription factor FOXO3A which is also known for its implication in autophagy regulation. Many studies highlighted the key role of autophagy in the ovary at different stages of folliculogenesis and particularly in PMF survival.

Through an *in vitro* approach with organotypic cultures of prepubertal mouse ovaries, treated or not with AMH, we aimed to understand the link between AMH, autophagy and FOXO3A transcription factor. Autophagy and FOXO3A phosphorylation were analyzed by western blot. The expression of genes involved in autophagy was quantified by RT-qPCR. We confirmed in our *in vitro* model the FOXO3A phosphorylation decrease and the induction of autophagy in ovaries incubated with AMH. AMH also induces the expression of genes involved in autophagy. Interestingly, most of these genes are known to be FOXO3A target genes. In conclusion, we have identified a new role for AMH namely the induction of autophagy, probably through FOXO3A activation. Thus, AMH protects the ovarian reserve by inhibiting the growth of PMF, but also by enabling their survival through activation of autophagy.

Keywords : AMH, autophagy, FOXO3A, primordial follicle, ovarian reserve.

Introduction

The ovarian reserve is built up during fetal life in women (1). The reserve pool is composed of quiescent primordial follicles (PMF) resulting from the association of diplotene oocytes surrounded by pregranulosa cells (1). PMF are activated to begin follicular growth from fetal life in humans or during neonatal period in rodents and this recruitment persists throughout reproductive life (until menopause in women) (2). The reserve pool is finely regulated by molecules implicated in follicular activation or PMF survival (3).

Phosphatidylinositol 3-kinase (PI3K) signaling pathway plays a crucial role in PMF recrutment (4). Its activation by different ligands such as Kit results in a phosphorylation cascade within the oocyte leading to follicular growth. Among this cascade, the transcription factor FOXO3A is phosphorylated, transported from the nucleus to the cytoplasm, utilizing the 14-3-3 molecular chaperone, and degraded by proteasomes after polyubiquitinisation (5). Anti-Müllerian hormone (AMH) is a glycoprotein of the TGF-β family expressed by granulosa cells and produced by growing follicles, ranging from the primary stage of development to reach its maximum at preantral and small antral stage (6). AMH is known to inhibit the initial PMF recruitment (6–8).

The maintenance of the reserve pool is therefore dependent on the survival of PMF. Atresia is the fate of 99% of follicles, including PMF (9). Several studies have highlighted the key role of autophagy in this survival (9–11). Autophagy is an intracellular lysosomal-dependent degradative process of cytoplasmic components and defective organelles, phylogenetically conserved from yeast to mammals (9, 12). This process is observed in all cells at basal state and is induced in case of stress like starvation (13). Autophagy is tightly regulated at multiple levels and autophagy-related (ATG) proteins are key players in this process. Autophagy proceeds in five successive steps, namely initiation, nucleation, expansion, maturation, and degradation (14). Autophagy induction results in the formation of a double membrane, the phagophore, which sequesters part of the cytoplasmic

content. This phagophore expands and closes to form a vacuole called autophagosome. The autophagosome then fuses with a lysosome to form an autolysosome in which acid hydrolases degrades the sequestered material. In the ovary, autophagy is also involved at different stages of folliculogenesis from the formation of reserve pool to follicular atresia and corpus luteum regression (15–17).

Although autophagy plays a key role in the PMF resting pool, the underpinning mechanisms are not clearly understood. In a recent *in vivo* study, we obtained data suggesting that injection of AMH into mouse induces autophagy and we showed that AMH activated the FOXO3A transcription factor (18).This factor is also known to be a regulator of autophagy (19). Based on these observations, we hypothesized that AMH protects the PMF pool by both inhibiting follicular activation and inducing autophagy. Using a mouse ovary organotypic culture, we studied the link between AMH, FOXO3A and autophagy.

Materials and Methods

Animals

Three-week-old C57BL6 weaned female mice (Janvier Labs) were acclimated during 5 days under conditions of constant temperature (21 ± 2°C), humidity (min. 50%), and lighting (12-h light/dark, lights on at 7 a.m) with *ad libitum* access to food and water (deionized).

The animal facility was granted approval (No. D94-043-12) by the French administration (Ministère de l'Agriculture). All procedures were approved by the local ethic committee Consortium des Animaleries Paris Sud (CAPSud). For organotypic culture, mice were euthanized at 26 post-natal days and ovaries were removed.

Organotypic culture

Ovaries were incubated in 5% CO_2 at 37°C into cell culture inserts (12 mm diameter, polycarbonate membrane, 0.4 µm pore size, Transwell, Corning) with Dulbecco's Modified Eagle Medium

(DMEM/F12) supplemented with 1% glutamine, 1% sodium pyruvate (100 mM), 0.3% bovine serum albumin, 1% penicillin/streptomycin and 5.6 µg/mL transferrin. Murine recombinant AMH (1 µg/mL) was added when necessary (*M. musculus* recombinant AMH, CliniSciences, Signalway Antibody).

Antibodies

Antibodies directed against actin (clone C4, Millipore, 1/5000 PBST-1% milk), Smad 1 (#6944, Cell Signaling, 1/500-TBST-1% milk), Phospho-Smad1/5 (Ser463/465, #9516, Cell Signaling, 1/1000-TBST-5% BSA), Phospho-FOXO3A (Ser318/321, #9465, Cell Signaling, 1/1000-TBST-5% BSA), FOXO3A (#2497, Cell Signaling, 1/500-TBST-5% milk), LC3 (L7543, Sigma-Aldrich, 1/2000-PBST-1% milk), Ulk1 (D8H5, Cell Signaling 8054, 1/500, TBST 5% BSA), Wipi2 (Sigma SAB4200399, 1/500, PBST 1% Lait), Atg16L1 (MBL PM040, 1/1000, PBST 1% lait), Atg5 (Cell Signaling 12994, 1/1000, TBST5% BSA) were used for western-blot analysis. Antibodies directed against FOXO3A (#2497, Cell Signaling, 1/50 PBS 0.5%BSA) and LC3 (PM036, MBL, 1/1000-20mM Hepes/135mM NaCl/1% BSA) were used for immunofluorescence analysis. Horseradish peroxidase-linked secondary antibodies (Jackson ImmunoResearch) or immunofluorescent antibodies anti-mouse or anti-rabbit (Invitrogen) were used for protein gel blot analysis.

Immunofluorescence

Ovaries were dissected and fixed in 4% paraformaldehyde, washed, embedded in paraffin, and sectioned. The ovaries were cut 4 µm thick and mounted on slides. Sections were deparaffinized and rehydrated. After epitope retrieval treatment (at 90°C for 30min in citrate buffer solution 1X, pH 6.0; Dako, Glostrup, Denmark), nonspecific binding sites were blocked for 1 h and the sections were incubated with appropriate primary antibodies overnight at 4°C. The sections were washed in PBS and then incubated for 1 h with appropriate secondary antibodies. After washing, the sections were finally incubated with DAPI for 5 min for fluorescent detection of nuclei morphology. All sections were rinsed in PBS for 5 min, air dried, and coverslipped using fluorescence mounting medium

(Dako). The tissue sections were then examined by confocal microscopy (SP5 Leica Confocal Microscope, Leica Microsystems, Deerfield, IL, USA) or digital whole-slide high-resolution images was capture using The Panoramic 250 Flash Slide Scanner system (3DHistech, Budapest, Hungary with a 340 Plan-Apochromat objective and a 31.6 camera adapter magnification).

Western blot analysis

Ovaries were homogenized in 65 mM Tris, pH 6.8, 4% SDS, 1.3% β-mercapto-ethanol, phosphatase and protease inhibitors (Sigma-Aldrich) using a TissueLyser LT homogenizer (Qiagen). Samples were held at 100°C for 8 min. After SDS-PAGE, the proteins were electrotransferred onto a PVDF or a nitrocellulose membrane. For immunoblotting, the membranes were probed overnight with relevant antibodies and then incubated with appropriated fluorescent or horseradish peroxidase–linked secondary antibodies. Bound immunoglobulins were revealed by fluorescence or chemiluminescent detection (Immobilon™ Western, Millipore). Membranes were scanned with Odyssey imaging system (Li-Cor) and quantification was conducted using Image Studio 5.2 software (Li-Cor). All western blots shown are representative of 3 to 8 experiments.

Real-time reverse-transcription quantitative polymerase chain reaction (RT-qPCR)

Total RNA were extracted from ovaries using the TRI Reagent® (Molecular Research Center, Inc), according to the manufacturer's recommendations. First strand cDNA was synthesized using the High Capacity cDNA Reverse Transcription kit (Applied Biosystems). RT-qPCR was performed on a QuantStudio 6 Flex System (Applied Biosystems). Threshold cycle (Ct) values were calculated using the second derivative maximum algorithm provided by the QuantStudio 6 software. To compensate for variations in the RNA input and in the efficiency of the RT-qPCR, we used a normalization strategy based on the housekeeping genes GAPDH and 36B4. Primer sequences are shown in Table 1. *Atg2a, Atg5, Becn1, Bnip3, Ulk1, Wipi2* and *Zfyve1* sequences are extracted from Audesse *et al* (20). The

results are expressed as means ± standard error of the mean (SEM) of 2 independent experiments with quadruplicate.

Statistical analysis

All results are expressed as means ± standard error of the mean (SEM). Statistical analyses (nonparametric t test (Mann-Whitney test) for 2-group comparisons and One-way ANOVA with Kruskal-Wallis posttest for multiple comparisons) were performed by GraphPadPrism (GraphPad Software Inc).

Results

AMH decreases FOXO3A phosphorylation

Organotypic ovarian cultures were used to study *in vitro* AMH signalling. We treated organotypic cultures with and without AMH. First, we confirmed AMH activity, since the Smad phosphorylation was induced after 15 min and 30 min incubation with AMH (Fig 1A). To highlight the transcription factor FOXO3A activation, we studied the expression of FOXO3A and its phosphorylated form (inactive) after 3 and 6 hours AMH treatment. We observed a decreased phosphorylation of FOXO3A (Fig 1B-C) and a significant decrease of P-FOXO3A/FOXO3A ratio (Fig 1B-D).

In oocytes, phosphorylated FOXO3A is located in the cytoplasm, then translocated in the nucleus after dephosphorylation to induce the expression of target genes. To study FOXO3A localization after AMH treatment, we performed immunofluorescence analysis on ovarian sections (Fig. 1E). In PMF oocyte, FOXO3A is located mainly in the cytoplasm in absence of AMH, while after 3h AMH incubation FOXO3A is both cytoplasmic and nuclear.

AMH induces autophagy in ovary

We thus showed that AMH leads to an increase of dephosphorylated FOXO3A active form which is subsequently translocated in the nucleus to exert its transcription activity. As FOXO3A is known to be

an actor of autophagy regulation in different tissues (20–23), we next analyzed autophagy modulation by AMH in our *in vitro* model.

First, the localization of LC3 a widely-used marker protein that is recruited to the autophagosomal membrane, was analyzed by immunofluorescence staining of tissue sections of ovaries treated or not with AMH. It reveals the appearance of a large number of autophagic puncta in oocytes within primordial follicles of AMH-treated ovaries compared to control ovaries (Fig. 2A).

To better quantify autophagosomes, LC3 protein was analyzed by western blot in total extracts of ovaries incubated with or without AMH and 100 µM chloroquine (CQ) for 13 hours (Fig. 2B). This protein exists in two molecular forms, LC3-I and LC3-II. When autophagy is induced, the LC3-I form is cleaved and conjugated to phosphatidyl-ethanolamine (PE) to give the LC3-II form which is associated with the autophagosome membrane. The expression level of the LC3-II protein is therefore correlated with the autophagosome number. CQ is a lysosomotropic agent which inhibits fusion between autophagosomes and lysosomes and allows to evaluate autophagosome biosynthesis.

After 13 hours of treatment with AMH and CQ, we observed a 80% increase of LC3-II compared to ovaries treated with CQ alone, indicating an increase in autophagosome biosynthesis (Fig. 2B and C). To assess the autophagic flux, which reflects the entire process of autophagy including both biosynthesis and degradation of autophagosomes, we calculate the ratio LC3-II CQ+/LC3-II CQ- in the AMH-treated and untreated groups. The flux is increased by about 40% in the ovaries treated with AMH for 13 hours, as compared to the control ovary cultures (Fig. 2D).

We also measured by western-blot the expression of the polyubiquitin-binding protein p62 (sequestosome 1), a common autophagy substrate (Fig.2B). p62/ SQSTM1 protein level is reduced by about 25% in AMH-treated ovaries compared to control ovaries (Fig. 2B and C).

Taken together, these results indicate that AMH induces autophagy in ovarian culture.

AMH increases the expression of genes involved in autophagy

To decipher the underlying mechanisms by which AMH induces autophagy, we studied the expression of FOXO3A target autophagy genes involved in different stages of autophagy by RT-qPCR.

After 3h of AMH treatment, we observed a significant increase of *Atg16l1, Gabarapl2, Wipi2*, *Atg2a*, *Ulk1, Zfyve1* and *Atg5* genes expression, ranging from 25% to 50% as compared to the control group (Fig. 3). This significantly increase persists after 6h of incubation for *Atg16l1, Gabarapl2* and *Wipi2*. In contrast, the expression of *Atg2a, Zfyve1, Atg5* and *Ulk1* tends to return to the level of the control group after 6h of incubation with AMH. The expression of *Atg2b* is stagnant at 3h and increases significantly at 6h.

We studied the protein expression of UlK1, Wipi2, Atg16L1 and Atg5 in protein extracts from ovaries treated or not with AMH for 6h. We thus showed that increased expression of their genes correlated well with an increase in their protein expression (Fig. 4).

Taken together, AMH induces autophagy in ovary by increasing the expression of a number of genes involved in this process.

Discussion

AMH is a well-known key regulator of ovarian follicular growth. This role was highlighted in AMH *null* female mice which exhibited an increased number of growing follicles (pre-antral follicles and small antral follicles) and a reduced number of PMF at 4 months of life compared to the control population (7). In the same manner, disruption of AMHR2 signaling leads to a phenotype similar to *Amh*-deficient mice with persistence of the Müllerian ducts and premature depletion of the follicular pool (6, 24). Moreover in women, mutation of *AMHR2* is responsible for clinical presentation of primary ovarian insufficiency (POI) (25–27). To date, the mechanism by which AMH inhibits follicle growth remains unknown. In the present study, we show that AMH decreases FOXO3A phosphorylation in organotypic ovarian cultures and induced its nuclear translocation, confirming our previous *in vivo* observation in pubescent mice injected with exogenous recombinant AMH (18).

In adult female, most PMF are quiescent. Foxo3A plays a crucial role in maintaining this dormancy, which is necessary to preserve the ovarian reserve and maintain the reproductive capacity of mammals (28). *Foxo3a null* female mice are sterile from 15 weeks of life due to complete follicular loss (29). Conversely, *Foxo3*-transgenic mice, with FOXO3 overexpression, present a larger PMF count than wild-type mice (30). Thus, FOXO3A signaling inhibits PMF activation, maintaining them into their initial state, preserving thereby the follicular reserve. The decreased FOXO3A phosphorylation and its nuclear translocation after AMH treatment suggest that inhibition of follicular growth by AMH may involve FOXO3A signaling.

FOXO3A is also involved in autophagy regulation. FOXO3A induces expression of autophagy genes in several cell models. In neural stem cells, Audesse *et al* identified FOXO3A target genes based on ChIP-seq analysis (20). Through inactivation or overexpression of FOXO3A, they confirmed *Wipi2*, *Atg2a*, *Atg5*, *Bnip3*, *Ulk1*, *Zfyve1*, *Atg10* and *Pink1* as FOXO3A target genes in this cellular model. *Bnip3* as target gene was confirmed in hematopoietic stem cells (23). Zhao *et al* and Mammucari *et al* studied FOXO3A target genes in muscle cells and identified two additional genes : *LC3* and *Becn1* (21, 22). In the current study we demonstrate that AMH induces an increase in autophagosome biosynthesis and autophagic flux in ovaries. Moreover, expression of *Ulk1, Atg2a*, *Atg2b, Atg5*, *Becn1, Gabarapl2, Atg16l1, Wipi2* and *Zfyve1*, autophagy genes involved at different stages of autophagy and controlled by FOXO3 at the transcriptional level (20, 21, 31, 32), was significantly increased in AMH treated ovaries. These results strongly suggest that AMH induces autophagy in the ovary though FOXO3A signaling.

Autophagy is known to be crucial in PMF pool preservation. In fact, germ cell-specific *Atg7* knockout in female mice lead to severely subfertility with a significant decline of PMF pool at 6 months of age (10). In the same manner, compromised autophagy within the perinatal ovary, through the loss of *Becn1* or *Atg7*, also results in the premature loss of female germ cells (11). Along this line we have demonstrated that *ATG7* and *ATG9* loss-of-function variants were involved in the pathogenesis of POI in women (33).

In our previous study (18), we showed that *in vivo* AMH injection to mice, results in an increase in PMF number which is in accordance with studies showing an increased number of PMF after caloric restriction or rapamycin treatment which both induce autophagy (34, 35).

Thus, we can conclude that AMH plays a crucial role in follicular pool preservation. We propose that AMH has two combined actions both mediated by FOXO3A signaling, the first one by inhibiting follicular activation and second one by activating autophagy, both actions contributing to the preservation of the ovarian reserve (Cf graphical abstract).

Data Availability statement

All study data are included in the article

Conflict of interest

The authors declare to have no competing interest.

Authors contributions

Isabelle Beau and Charlotte Sonigo designed research; Tatiana Lecot-Connan, Yasmine Boumerdassi, Françoise Magnin and Isabelle Beau performed the experiments; Tatiana Lecot-Connan, Yasmine Boumerdassi and Isabelle Beau analyzed data; Isabelle Beau, Charlotte Sonigo, Nadine Binart and Peter Kamenický discussed the results and Tatiana Lecot-Connan, Charlotte Sonigo and Isabelle Beau wrote the paper.

Acknowledgments

The authors thank L. Amazit, N. Ba and O. Trassard (Unité Mixte de Service 44 « Institut Biomédical du Val de Bièvre », Le Kremlin-Bicêtre, France) for assistance in confocal microscopy, histological proceedings, and slide scanning, respectively.

Funding

This work was supported by grants from “Agence de Biomédecine” and by the Institut National de la Santé et de la Recherche Médicale.

References

1. Kerr, J. B., Myers, M., and Anderson, R. A. (2013) The dynamics of the primordial follicle reserve. *Reprod. Camb. Engl.* **146**, R205-215
2. McGee, E. A. and Hsueh, A. J. (2000) Initial and cyclic recruitment of ovarian follicles. *Endocr. Rev.* **21**, 200–214
3. Reddy, P., Zheng, W., and Liu, K. (2010) Mechanisms maintaining the dormancy and survival of mammalian primordial follicles. *Trends Endocrinol. Metab. TEM* **21**, 96–103
4. Adhikari, D. and Liu, K. (2009) Molecular mechanisms underlying the activation of mammalian primordial follicles. *Endocr. Rev.* **30**, 438–464
5. Zhang, H., Lin, F., Zhao, J., and Wang, Z. (2020) Expression Regulation and Physiological Role of Transcription Factor FOXO3a During Ovarian Follicular Development. *Front. Physiol.* **11**, 595086
6. di Clemente, N., Racine, C., Pierre, A., and Taieb, J. (2021) Anti-Müllerian Hormone in Female Reproduction. *Endocr. Rev.* **42**, 753–782
7. Durlinger, A. L., Kramer, P., Karels, B., de Jong, F. H., Uilenbroek, J. T., Grootegoed, J. A., and Themmen, A. P. (1999) Control of primordial follicle recruitment by anti-Müllerian hormone in the mouse ovary. *Endocrinology* **140**, 5789–5796
8. Durlinger, A. L. L., Gruijters, M. J. G., Kramer, P., Karels, B., Ingraham, H. A., Nachtigal, M. W., Uilenbroek, J. T. J., Grootegoed, J. A., and Themmen, A. P. N. (2002) Anti-Müllerian hormone inhibits initiation of primordial follicle growth in the mouse ovary. *Endocrinology* **143**, 1076–1084
9. Bhardwaj, J. K., Paliwal, A., Saraf, P., and Sachdeva, S. N. (2022) Role of autophagy in follicular development and maintenance of primordial follicular pool in the ovary. *J. Cell. Physiol.* **237**, 1157–1170
10. Song, Z.-H., Yu, H.-Y., Wang, P., Mao, G.-K., Liu, W.-X., Li, M.-N., Wang, H.-N., Shang, Y.-L., Liu, C., Xu, Z.-L., Sun, Q.-Y., and Li, W. (2015) Germ cell-specific Atg7 knockout results in primary ovarian insufficiency in female mice. *Cell Death Dis.* **6**, e1589
11. Gawriluk, T. R., Hale, A. N., Flaws, J. A., Dillon, C. P., Green, D. R., and Rucker, E. B. (2011) Autophagy is a cell survival program for female germ cells in the murine ovary. *Reprod. Camb. Engl.* **141**, 759–765
12. Al-Bari, M. A. A. and Xu, P. (2020) Molecular regulation of autophagy machinery by mTOR-dependent and -independent pathways. *Ann. N. Y. Acad. Sci.* **1467**, 3–20
13. Kroemer, G., Mariño, G., and Levine, B. (2010) Autophagy and the integrated stress response. *Mol. Cell* **40**, 280–293
14. Kang, R., Zeh, H. J., Lotze, M. T., and Tang, D. (2011) The Beclin 1 network regulates autophagy and apoptosis. *Cell Death Differ.* **18**, 571–580
15. Zhou, J., Peng, X., and Mei, S. (2019) Autophagy in Ovarian Follicular Development and Atresia. *Int. J. Biol. Sci.* **15**, 726–737
16. Teeli, A. S., Leszczyński, P., Krishnaswamy, N., Ogawa, H., Tsuchiya, M., Śmiech, M., Skarzynski, D., and Taniguchi, H. (2019) Possible Mechanisms for Maintenance and Regression of Corpus Luteum Through the Ubiquitin-Proteasome and Autophagy System Regulated by Transcriptional Factors. *Front. Endocrinol.* **10**, 748
17. Kumariya, S., Ubba, V., Jha, R. K., and Gayen, J. R. (2021) Autophagy in ovary and polycystic ovary syndrome: role, dispute and future perspective. *Autophagy* **17**, 2706–2733

18. Sonigo, C., Beau, I., Grynberg, M., and Binart, N. (2019) AMH prevents primordial ovarian follicle loss and fertility alteration in cyclophosphamide-treated mice. *FASEB J. Off. Publ. Fed. Am. Soc. Exp. Biol.* **33**, 1278–1287
19. Ravikumar, B., Sarkar, S., Davies, J. E., Futter, M., Garcia-Arencibia, M., Green-Thompson, Z. W., Jimenez-Sanchez, M., Korolchuk, V. I., Lichtenberg, M., Luo, S., Massey, D. C. O., Menzies, F. M., Moreau, K., Narayanan, U., Renna, M., Siddiqi, F. H., Underwood, B. R., Winslow, A. R., and Rubinsztein, D. C. (2010) Regulation of mammalian autophagy in physiology and pathophysiology. *Physiol. Rev.* **90**, 1383–1435
20. Audesse, A. J., Dhakal, S., Hassell, L.-A., Gardell, Z., Nemtsova, Y., and Webb, A. E. (2019) FOXO3 directly regulates an autophagy network to functionally regulate proteostasis in adult neural stem cells. *PLoS Genet.* **15**, e1008097
21. Zhao, J., Brault, J. J., Schild, A., Cao, P., Sandri, M., Schiaffino, S., Lecker, S. H., and Goldberg, A. L. (2007) FoxO3 coordinately activates protein degradation by the autophagic/lysosomal and proteasomal pathways in atrophying muscle cells. *Cell Metab.* **6**, 472–483
22. Mammucari, C., Milan, G., Romanello, V., Masiero, E., Rudolf, R., Del Piccolo, P., Burden, S. J., Di Lisi, R., Sandri, C., Zhao, J., Goldberg, A. L., Schiaffino, S., and Sandri, M. (2007) FoxO3 controls autophagy in skeletal muscle in vivo. *Cell Metab.* **6**, 458–471
23. Warr, M. R., Binnewies, M., Flach, J., Reynaud, D., Garg, T., Malhotra, R., Debnath, J., and Passegué, E. (2013) FOXO3A directs a protective autophagy program in haematopoietic stem cells. *Nature* **494**, 323–327
24. Mishina, Y., Rey, R., Finegold, M. J., Matzuk, M. M., Josso, N., Cate, R. L., and Behringer, R. R. (1996) Genetic analysis of the Müllerian-inhibiting substance signal transduction pathway in mammalian sexual differentiation. *Genes Dev.* **10**, 2577–2587
25. Qin, C., Yuan, Z., Yao, J., Zhu, W., Wu, W., and Xie, J. (2014) AMH and AMHR2 genetic variants in Chinese women with primary ovarian insufficiency and normal age at natural menopause. *Reprod. Biomed. Online* **29**, 311–318
26. Yoon, S. H., Choi, Y. M., Hong, M. A., Kim, J. J., Lee, G. H., Hwang, K. R., and Moon, S. Y. (2013) Association study of anti-Mullerian hormone and anti-Mullerian hormone type II receptor polymorphisms with idiopathic primary ovarian insufficiency. *Hum. Reprod. Oxf. Engl.* **28**, 3301–3305
27. Li, L., Zhou, X., Wang, X., Wang, J., Zhang, W., Wang, B., Cao, Y., and Kee, K. (2016) A dominant negative mutation at the ATP binding domain of AMHR2 is associated with a defective anti-Müllerian hormone signaling pathway. *Mol. Hum. Reprod.* **22**, 669–678
28. Moniruzzaman, M. and Miyano, T. (2010) Growth of primordial oocytes in neonatal and adult mammals. *J. Reprod. Dev.* **56**, 559–566
29. Castrillon, D. H., Miao, L., Kollipara, R., Horner, J. W., and DePinho, R. A. (2003) Suppression of ovarian follicle activation in mice by the transcription factor Foxo3a. *Science* **301**, 215–218
30. Pelosi, E., Omari, S., Michel, M., Ding, J., Amano, T., Forabosco, A., Schlessinger, D., and Ottolenghi, C. (2013) Constitutively active Foxo3 in oocytes preserves ovarian reserve in mice. *Nat. Commun.* **4**, 1843
31. Guan, S., Chen, X., Chen, Y., Wan, G., Su, Q., Liang, H., Yang, Y., Fang, W., Huang, Y., Zhao, H., Zhuang, W., Liu, S., Wang, F., Feng, W., Zhang, X., Huang, M., Wang, X., and Zhang, L. (2022) FOXO3 mutation predicting gefitinib-induced hepatotoxicity in NSCLC patients through regulation of autophagy. *Acta Pharm. Sin. B* **12**, 3639–3649
32. Grossi, V., Fasano, C., Celestini, V., Lepore Signorile, M., Sanese, P., and Simone, C. (2019) Chasing the FOXO3: Insights into Its New Mitochondrial Lair in Colorectal Cancer Landscape. *Cancers* **11**, E414
33. Delcour, C., Amazit, L., Patino, L. C., Magnin, F., Fagart, J., Delemer, B., Young, J., Laissue, P., Binart, N., and Beau, I. (2019) ATG7 and ATG9A loss-of-function variants trigger autophagy impairment and ovarian failure. *Genet. Med. Off. J. Am. Coll. Med. Genet.* **21**, 930–938

34. Luo, L.-L., Chen, X.-C., Fu, Y.-C., Xu, J.-J., Li, L., Lin, X.-H., Xiang, Y.-F., and Zhang, X.-M. (2012) The effects of caloric restriction and a high-fat diet on ovarian lifespan and the expression of SIRT1 and SIRT6 proteins in rats. *Aging Clin. Exp. Res.* **24**, 125–133
35. Zhang, X., Li, L., Xu, J., Wang, N., Liu, W., Lin, X., Fu, Y., and Luo, L. (2013) Rapamycin preserves the follicle pool reserve and prolongs the ovarian lifespan of female rats via modulating mTOR activation and sirtuin expression. *Gene* **523**, 82–87

385 **Figure Legends**

386

387 **Figure 1. AMH decreases FOXO3A phosphorylated form.** Ovaries were incubated in the presence or
388 absence of 1 µg/mL AMH for 3 and 6 hours. A) Representative western-blot analysis of P-Smad1/5,
389 Smad1 and Actin proteins in the control group and after 15 and 30 min incubation with AMH and P-
390 Smad/Smad ratio. B) Representative western blot analysis of P-FOXO3A, FOXO3A and Actin proteins
391 in the control group and after 3 and 6 hours incubation with AMH. C) and D) The graphs represent
392 the P-FOXO3a/actin and P-FOXO3A/FOXO3 ratio at the different time points. Data represent the
393 mean ± SEM of at least 3 independent experiments (*p<0.05, **p<0.01, ***p<0.001, ****p<0.0001
394 Kuskal-Wallis test). E) Histologic analysis of FOXO3A localization in PMF from ovaries incubated or
395 not with AMH for 3 hours. Ovarian sections were immunostained with an antibody against FOXO3A
396 (red). Nuclei were labelled with Dapi (blue). Images were taken on a Leica SP5 confocal microscope.
397 Bar scale : 10µm.

398

399 **Figure 2. AMH induces autophagy.** Ovaries were incubated in the presence or absence of 1 µg/mL
400 AMH and 100 µM CQ for 13 hours. A) Immunofluorescence analysis of autophagosomes in ovaries
401 incubated or not with AMH for 13 hours. Ovarian sections were immunostained with an antibody
402 against LC3 (red). Nuclei were labelled with Dapi (blue). Images were taken from scanned slides. Bar
403 scale : 10µm. B) Ovary lysates were subjected to immunoblotting analyses using anti-p62, anti-LC3
404 and anti-actin antibodies. C) and D) The graph represents the p62/Actin, LC3-II/Actin ratio and the
405 autophagic flux. Data represent the mean ± SEM of 8 independent experiments. *p<0.05, ** p < 0,01,
406 by Mann-Whitney test. D)

407

408 **Figure 3. AMH increases the expression of genes involved in autophagy.** Ovaries were incubated in
409 the presence or absence of 1 µg/mL AMH for 3 and 6 hours. Total RNA were extracted and quantified

by RT-qPCR. Results are expressed as the relative amount of ΔCt, between control and treated ovaries, normalized to the mean ΔCt of two housekeeping genes, GAPDH and 36B4. These results are from two experiments, in which each condition was represented in quadruplicate. Error bars represent SEM and dots represent values distribution. *p < 0.05, ** p < 0.01, *** p < 0.001, **** p < 0.0001, by Kruskal-Wallis test.

Figure 4: AMH increases the expression of Ulk1, Wipi2, Atg16L1 and Atg5. Ovaries were incubated in the presence or absence of 1 µg/mL AMH for 6 hours. Ovary lysates were subjected to immunoblotting analyses using anti-Ulk1, anti-Wipi2, anti-Atg16L1 anti-Atg5 and anti-actin antibodies. The band corresponding to each Atg protein was quantified and normalized against actin used as a loading control (Atg/actin).

Figure 1

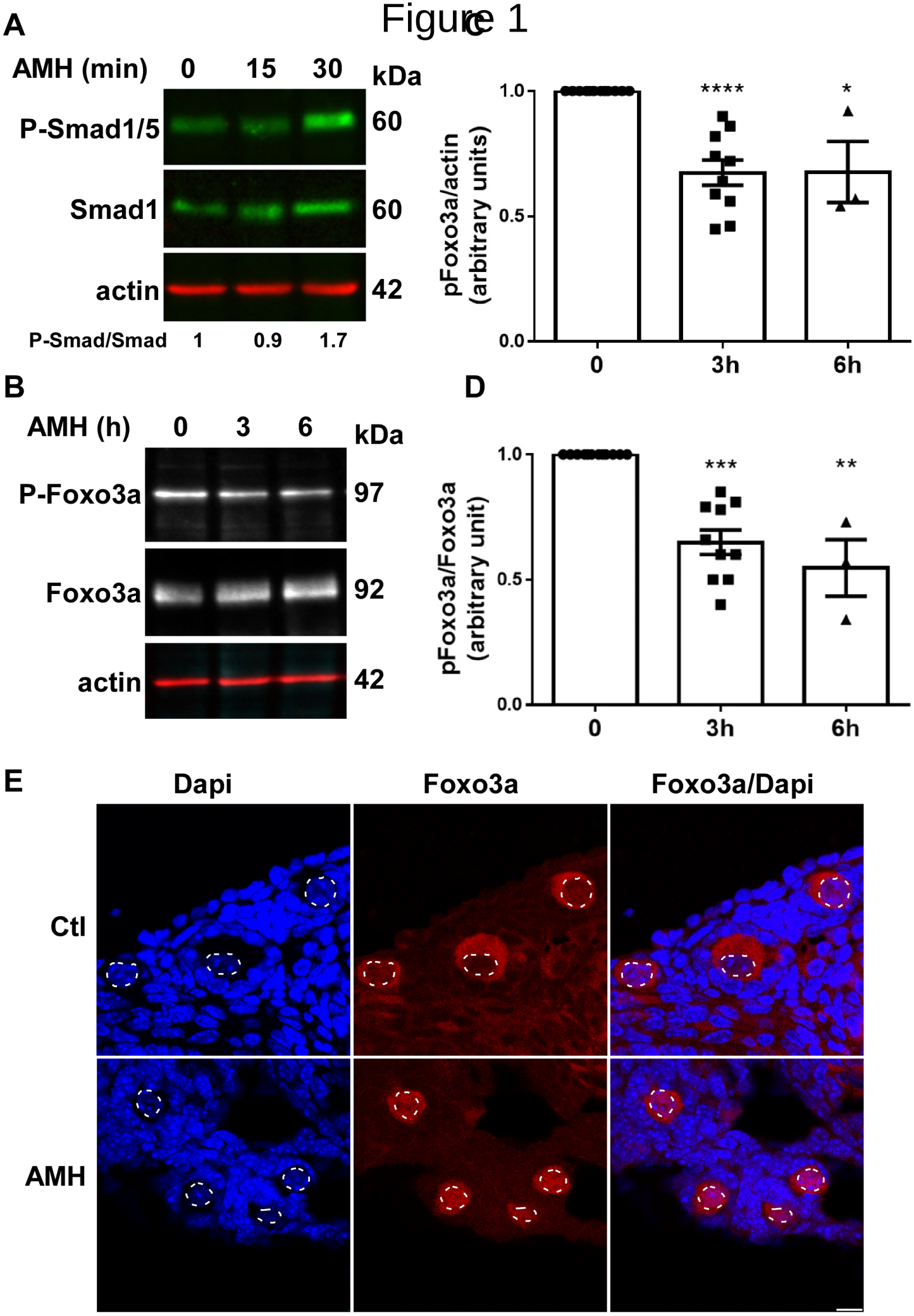
A
AMH (min) 0 15 30 kDa
P-Smad1/5 60
Smad1 60
actin 42
P-Smad/Smad 1 0.9 1.7
C
pFoxo3a/actin (arbitrary units)
1.0
0.5
0.0
****
*
0
3h
6h
B
AMH (h) 0 3 6 kDa
P-Foxo3a 97
Foxo3a 92
actin 42
D
pFoxo3a/Foxo3a (arbitrary unit)
1.0
0.5
0.0
***
**
0
3h
6h
E
Dapi
Foxo3a
Foxo3a/Dapi
Ctl
AMH

Figure 2

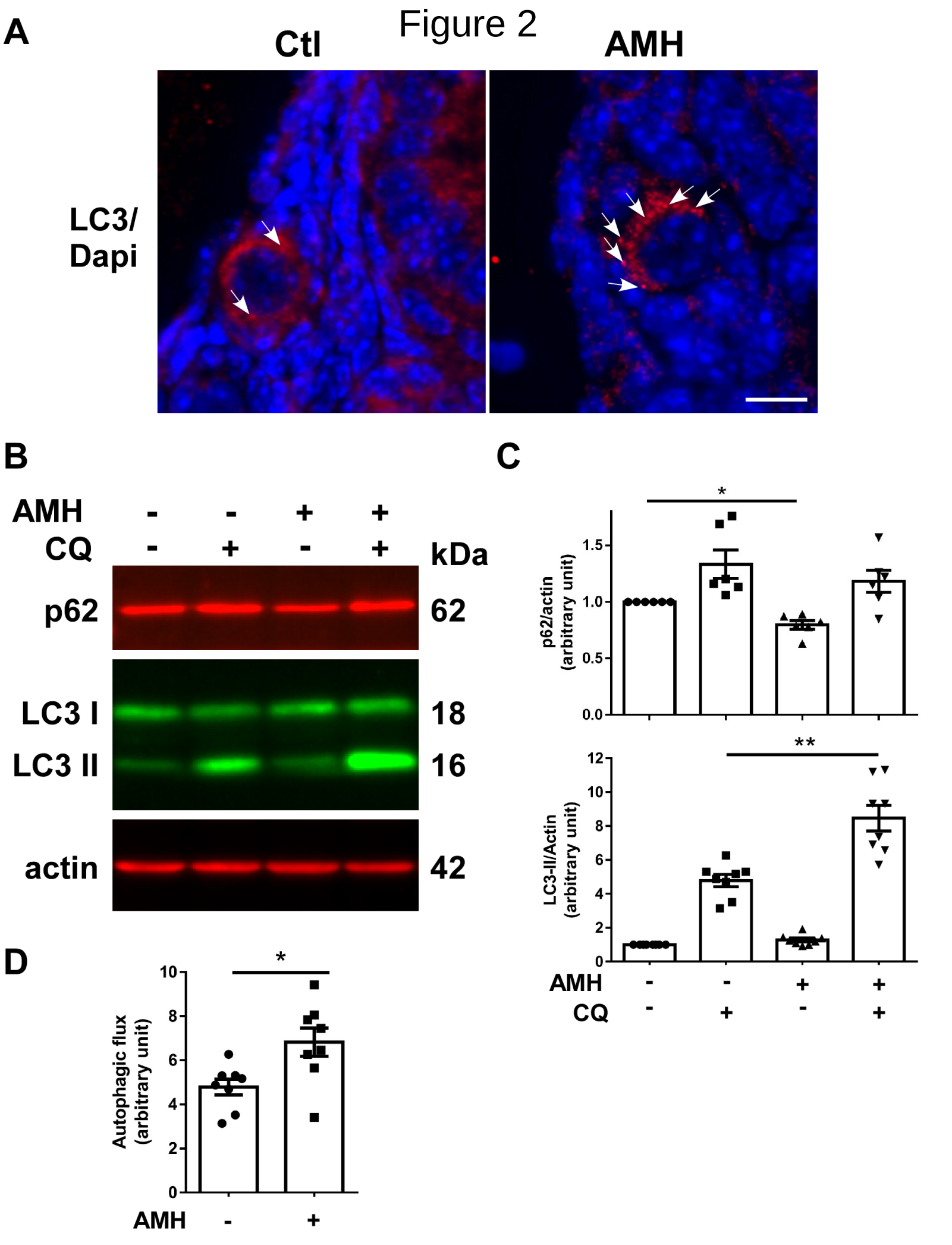
A
Ctl
AMH
LC3/
Dapi
B
AMH - - + +
CQ - + - +
kDa
p62
62
LC3 I
LC3 II
18
16
actin
42
C
p62/actin
(arbitrary unit)
1.5
1.0
0.5
0.0
*
LC3-II/Actin
(arbitrary unit)
12
10
8
6
4
2
0
**
AMH - - + +
CQ - + - +
D
Autophagic flux
(arbitrary unit)
10
8
6
4
2
0
*
AMH - +

Figure 3

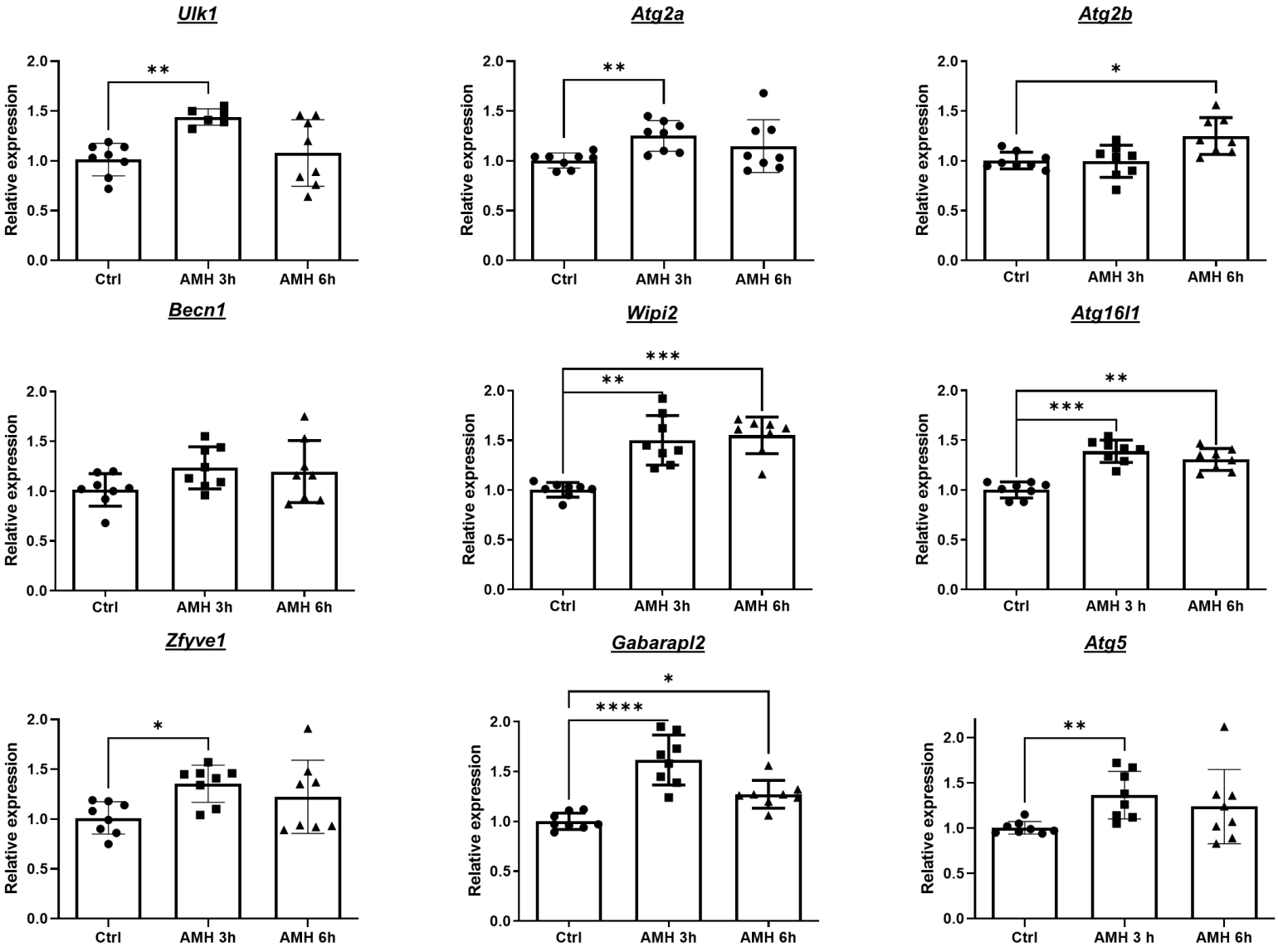
Ulk1
Atg2a
Atg2b
Becn1
Wipi2
Atg16l1
Zfyve1
Gabarapl2
Atg5
Relative expression
Ctrl
AMH 3h
AMH 6h
AMH 3 h
**
*
***
****

Figure 4

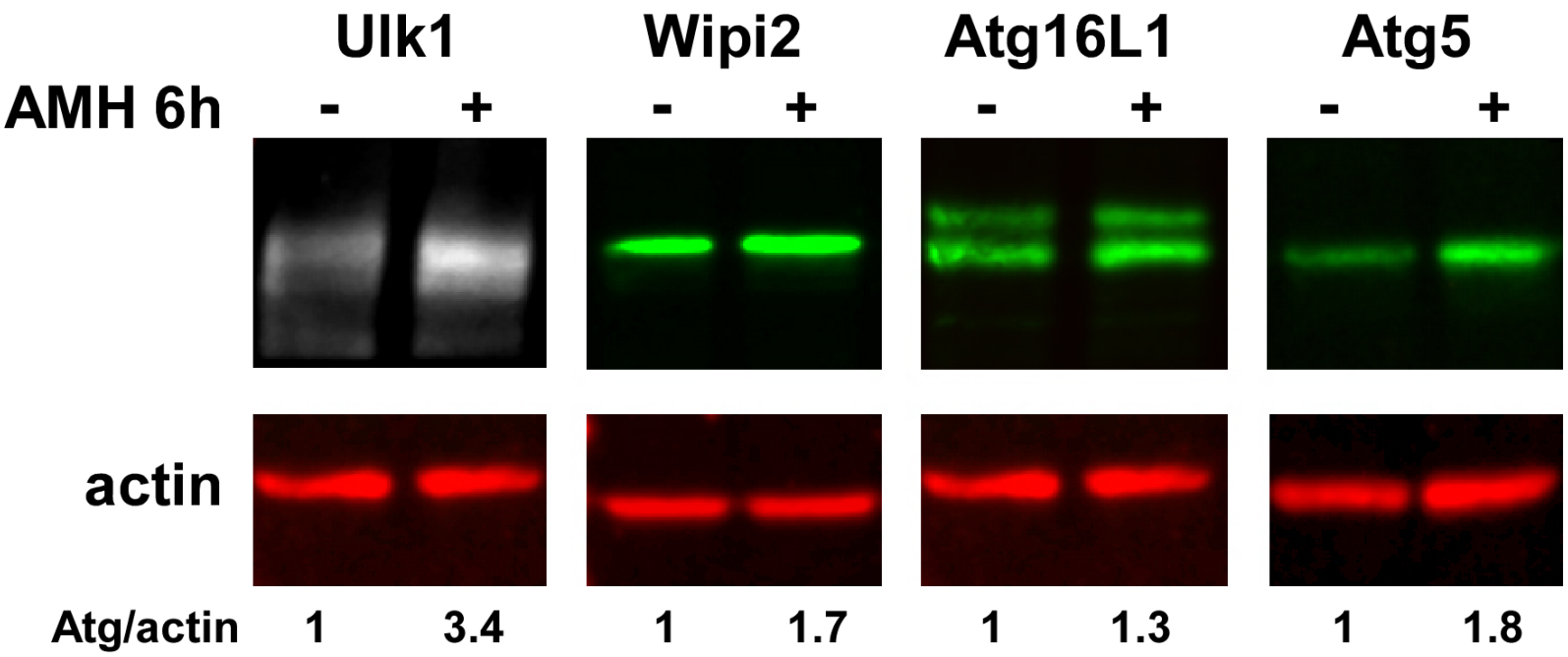
Ulk1
Wipi2
Atg16L1
Atg5
AMH 6h
- + - + - + - +
actin
Atg/actin
1 3.4 1 1.7 1 1.3 1 1.8

Table 1

Gene	Forward primer sequence	Reverse primer sequence
Atg2a	GGCATGGCTAAGGCTTATGA	TCAGTCCCTTCTGCTCATGG
Atg2b	CAAAATCTTCCCCCGTGTGT	AGTTGTGGGTGTGGCTCATAAA
Atg5	GATGGACAGCTGCACACACT	TTGGCTCTATCCCGTGAATC
Atg9b	TCCTTCGCTGCGTGGATTAC	CGAGGGTAGAATGGCATCTGA
Atg16l1	TTTTCAGGGCTGGTGGTATGT	AGGAAGGGAGTTCAGGGTTCTG
Becn1	TGTGTGCAGCAGTTCAAAGA	CACTGCCTCCAGTGTCTTCA
Bnip3	TTCTGAAGGTTTTCCTTCCATC	TTCATCAGAAGGTGCTAGTGGA
Gabarapl2	ACAGTCCCACAGTCCAGCCTAA	CTCTCCGCTGTAGGCCACAT
Ulk1	CCAGGCAGACATTGAGAACA	GTTGGCAGCAGGTAGTCAGG
Wipi2	GTGCCTATGTGCCCTCGT	ATCCTCTAGGCATGCACCAC
Zfyve1	CCGTGCAGAACACCTTGG	GTGCAGGATCTCATGGTCAG